

MBE growth of *para*-hexaphenyl on GaAs(001)-2 × 4

B. Müller ^{a,b,*}, T. Kuhlmann ^a, K. Lischka ^a, H. Schwer ^c, R. Resel ^d, G. Leising ^c

^a Universität—GH Paderborn, Fachbereich Physik, D-33095 Paderborn, Germany

^b Institut für Quantenelektronik, Nichtlineare Optik, ETH Zürich, CH-8093 Zürich, Switzerland

^c Laboratorium für Festkörperphysik, ETH Zürich, CH-8093 Zürich, Switzerland

^d Technische Universität Graz, Institut für Festkörperphysik, A-8010 Graz, Austria

Received 5 March 1998; accepted for publication 1 September 1998

Abstract

The morphology of *para*-hexaphenyl (PHP) grown on GaAs(001) by molecular beam epitaxy has been studied using atomic force microscopy (AFM). For elevated substrate temperatures between 90 and 170°C and a deposition rate of 0.7 Å s⁻¹, it was found that hexaphenyl on GaAs(001)-2 × 4 forms well-defined, three-dimensional islands of a rectangular shape oriented in <100>. Their constant width indicates that PHP is epitaxially grown as a coherently strained organic material. The island density shows the Arrhenius behavior resulting in activation barrier of (0.90 ± 0.04) eV. The normalized island size distributions closely resemble that of a critical island size of one. On the basis of the AFM measurements, X-ray diffraction data, and geometrical considerations, we developed a structural model for PHP grown on GaAs(001). © 1998 Elsevier Science B.V. All rights reserved.

Keywords: Atomic force microscopy; Gallium arsenide; Hexaphenyl; Molecular beam epitaxy; Surface morphology; Nucleation

1. Introduction

Advances in manufacturing of high-purity organic semiconductors promise to open a new frontier in the realization of blue-light emitting devices. Recently, such devices have been produced on the basis of *para*-hexaphenyl (PHP), a material that shows blue electroluminescence and can be easily evaporated in ultra-high vacuum by molecular beam Knudsen sources [1,2]. Well-defined growth conditions are important to maintain a high quantum efficiency since impurities and structural defects act as recombination centers. Moreover, defects can significantly limit the life-

time of organic devices, because a constant electric field over the whole film is no longer guaranteed. Therefore, molecular beam epitaxy (MBE) is a method of choice to produce high-quality organic thin films. For device applications, the organic layers are usually pure and flat but not free of defects. The applied growth conditions result in polycrystalline or even amorphous thin film structures. Higher substrate temperatures may lead to improved crystallinity, but they generally increase the surface roughness by island formation. The reason for this behavior can be related to the intermolecular bonding within the film that is stronger than the bonding between organic material and inorganic substrate. Hence, the MBE growth of organic compounds on well-defined inorganic semiconductor surfaces is interesting not only in terms of device technology but also in

* Corresponding author: Eidgenössische Materialprüfungs- und Forschungsanstalt, Abteilung Oberflächen- und Fügetechnik, CH-8600 Dübendorf, Switzerland.

terms of fundamentals in epitaxial growth. Besides silicon, GaAs(001) seems to be one of the most promising substrates for fundamental studies. GaAs(001) exhibits a sequence of surface reconstructions dependent on the substrate temperature and As/Ga flux ratio [3,4]. From a technological point of view, the As-rich (2×4)-reconstructed surface is dominant because thin film structures are frequently grown under these conditions, where many electronic properties are optimized. The surface of GaAs(001)- 2×4 has been intensively studied both theoretically and experimentally (see, for example, Refs. [5–7]), and is used for our deposition experiments.

GaAs has a lattice constant and crystal structure that differ drastically from PHP, and one would assume at first glance that PHP does not form well-defined and oriented islands, but rather randomly shaped conglomerates with many defects. The present communication demonstrates, however, that it is possible to produce well-ordered PHP on a suitable inorganic substrate, i.e. GaAs(001). In addition, we point out the similarities in MBE growth of PHP/GaAs(001) and simple atomic systems such as metals and semiconductors. The island density, island size distribution, and island shape have been analyzed. Although one may assume that the simple atomic models are not applicable to PHP/GaAs(001), e.g. due to the anisotropy of the molecular shape and the different interactions, the experimental results show identical behavior (Arrhenius behavior of the island density, scaling of the island size distribution, and spontaneous shape transition of coherently strained islands). Nevertheless, the obtained quantities cannot be interpreted by simple fundamental processes such as hopping diffusion, and the applicability of the models is still questionable. In this respect, our experimental study is a starting point for the detailed quantitative understanding of organic film growth on inorganic semiconductor surfaces.

2. Experimental

PHP, electrochemically synthesized [8], has been deposited in a home-made MBE-chamber under

ultra-high vacuum conditions. It was sublimated by means of a Knudsen-type MBE-source at a fixed source temperature of about 230°C. Before first deposition, the adsorbed water must be removed from the PHP. This process, performed by heating the source above 100°C for 24 h, was controlled by quadrupole mass spectrometry. It should be mentioned that PHP is thermally very stable. It does not dissociate below its isotropic melting point of 553°C [9]. Below the melting point, there are only different liquid-crystal phases at relatively high temperatures between 450 and 553°C, as verified by differential scanning calorimetry [10]. Therefore, we are sure that PHP sublimates as an intact molecule from the source at 230°C. Although PHP/GaAs with a monolayer thickness grown at a source temperature of 260°C and at a substrate temperature of 130°C are shown to be entire molecules [11], we cannot exclude any partial dissociation of PHP molecules at the GaAs interface, especially since the GaAs dangling bonds are known to be effective reaction sites.

Undoped GaAs(001) 2° misorientated towards $\langle 110 \rangle$ was used as substrate. However, we have not observed any influence of the preferential step direction due to the vicinality of the GaAs(001) surface on the island nucleation and the island morphology. Prior to growth, the substrate was heated to 680°C for 10 min under an As₄ pressure of 10^{-6} mbar (beam equivalent pressure) to remove the oxide. This procedure results in a (2×4)-reconstruction surface, as verified by reflection high-energy electron diffraction. It is well known that the (2×4) reconstructed surface can occur in different phases that are related to As coverages between 0.5 and 1 ML [5–7]. The RHEED pattern of the α -, β - and γ -phase are slightly different, but it was impossible to distinguish clearly between the phases with our RHEED system. The models for the (2×4) reconstruction on GaAs(001), however, are based on As-dimers without exception. Hence, the precise structure seems to be of minor importance in our study.

The substrate temperature was measured by a NiCr/Ni thermocouple calibrated by the melting points of In (157°C) and Pb (328°C). Atomic force microscopy (AFM) measurements on samples grown at relatively low growth temper-

atures, where desorption can be neglected, deliver a constant deposition rate of $(0.70 \pm 0.05) \text{ \AA s}^{-1}$.

The samples were characterized *ex situ* by atomic force microscopy (Topometrix Explorer) in non-contact- and contact mode. No significant differences between both modes were found. Hence, the PHP islands on GaAs(001) are mechanically quite stable. X-ray diffraction measurements have been performed on a STOE powder diffractometer using Ge-monochromatized $\text{CuK}_{\alpha 1}$ radiation. Secondary electron microscopy (SEM) and cathodoluminescence measurements were made using the electron microscope DSM 950 (Zeiss) using an electron energy of 4 keV.

3. Island shape of three-dimensional PHP islands on GaAs(001)

The growth of three-dimensional PHP islands on GaAs(001)- 2×4 is characterized in Fig. 1, showing a typical AFM image of PHP islands grown at a substrate temperature of 140°C and a deposition rate of 0.7 \AA s^{-1} . All islands exhibit an elongated shape and are oriented into the [100]

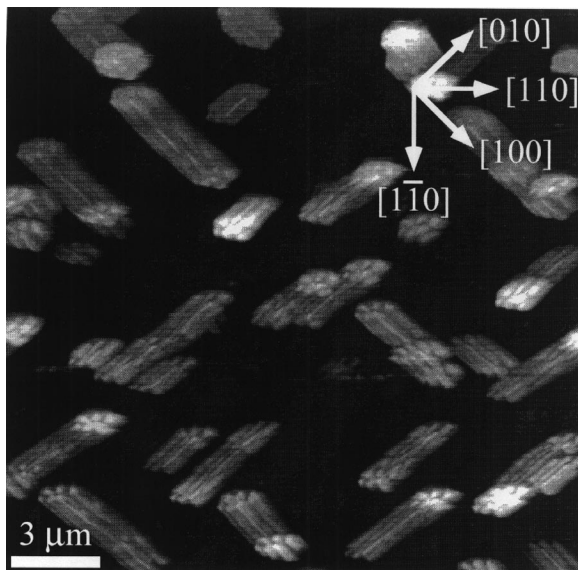


Fig. 1. AFM image characterizing the island morphology of PHP on GaAs(001) (substrate temperature during growth 140°C , deposition time 600 s at a flux rate of 0.7 \AA s^{-1} , average film thickness of 420 \AA).

and [010] direction with the same probability due to substrate symmetry. In heteroepitaxy, the formation of three-dimensional islands with defined facets can be energetically favorable; the underlying physical reasons are known from inorganic systems. Examples are given in the review by Venables et al. [12] The driving force for island formation in heteroepitaxy results from the minimization of the free energy, which has two major contributions. First, the intermolecular bonding within the substrate and film material as well as the interface bonding has to be taken into account. Three-dimensional islanding indicates strong bonding within film material and minor molecular interaction at the interface. The other contribution comes from the elastic strain energy, since flat surfaces of strained layers are unstable against undulations and shape changes.

The basis of the three-dimensional islands is almost rectangular, whereby the longer side is much straighter than the smaller side. The islands are about $1 \mu\text{m}$ wide and usually flat on top. The islands themselves may have an internal structure, as indicated by parallel stripes along the islands. As shown in Fig. 1, each island consists of five or six stripes. These stripes have a constant width of about 200 nm. Sometimes, they are not resolved due to the limited resolution of the AFM. However, the discussion here is restricted to the outer shape of the islands. The average height of the islands, $(1700 \pm 100) \text{ \AA}$, is four times larger than the average film thickness. The average film thickness of these three-dimensional crystallites corresponds to the film thickness of a two-dimensional thin film of identical volume that fully covers the substrate. After a deposition time of 600 s at a rate of 0.7 \AA s^{-1} , the average film thickness reached 420 \AA . The average height of the islands, however, is much greater.

In addition to the AFM experiments, we have performed secondary electron microscopy and cathodoluminescence measurements in order to exclude significant surface modifications by the AFM tip. The results of the three methods are compared to each other in Fig. 2. Although electron bombardment induces distinct damages, the nature of the interactions is different with respect to AFM. As the features of the images are

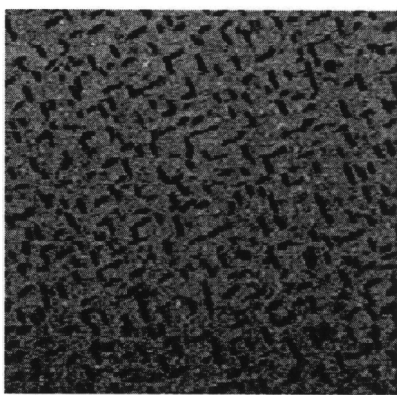
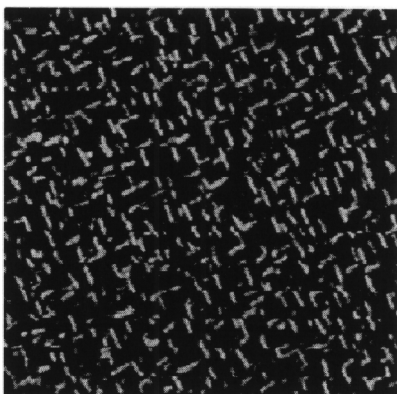
(a) AFM**(b) SEM****(c) Cathodoluminescence**

Fig. 2. Comparison between (a) AFM, (b) SEM, and (c) cathodoluminescence images showing the morphology of PHP on GaAs(001); image size: $100\ \mu\text{m} \times 100\ \mu\text{m}$; growth conditions see Fig. 1.

identical, we conclude that the AFM images present an unaffected picture of the surface morphology.

Cathodoluminescence is a very sensitive tool. For inorganic materials, it was demonstrated that a few monolayers can be easily observed [13]. The luminescence properties of organic films with a monolayer thickness depend on the dielectric constants of the film and substrate material as well as on the orientation of the molecules with respect to the substrate; a partial quenching can be observed [14]. Cathodoluminescence of PHP thin films has already been detected by the use of scanning tunneling microscopy (STM) [15,16]. Damages to PHP thin films under electron bombardment are minimized using low electron beam currents, whereby the choice of the electron energy is of minor importance. Studies at different energies are possible. Besides 290 eV [15], energies from 200 eV to 4 keV were used in the case of SEM (K. Popowitsch, G. Leising, pers. commun.), and 170 keV for electron energy loss spectroscopy [17].

Using cathodoluminescence, we were unable to find any PHP between the three-dimensional islands, and so the PHP film between the islands must be extremely thin, or even absent. Therefore, we have taken AFM images at regions where the substrate was partially shadowed by the tantalum holder (cp. Fig. 5a). These images do not show any contrast between the shadowed regions and the areas between the three-dimensional PHP islands. This means that PHP grows on GaAs(001)- 2×4 in the Vollmer–Weber or three-dimensional growth mode.

4. A novel structural model for PHP grown on GaAs(001)- 2×4

The island shape can be understood by a relatively simple model, which is motivated by the crystalline structure of PHP at room temperature [18]. Our model is based on X-ray diffraction data, AFM measurements, and geometrical considerations. The structure of PHP—sometimes called *p*-sexiphenyl, $\text{C}_{36}\text{H}_{26}$ —belongs to space group $\text{P}2_1/c$ and is similar to other oligomers. The lattice parameters at room temperature are found to be

$a=26.241 \text{ \AA}$, $b=5.568 \text{ \AA}$, $c=8.091 \text{ \AA}$ and $\beta=98.17^\circ$ [18]. The molecular axes of PHP are aligned within the (010)-plane, but not parallel to the a - and c -axes. They are stacked along b in a zigzag arrangement, forming an angle of 55° between the molecule plane and the (010)-face, as seen in Fig. 3b. In contrast to PHP deposited on glass, on silicon or on oxidized GaAs substrates, which, from X-ray diffraction shows only 001-reflections [11, 19], we were unable to observe any reflections of PHP grown on GaAs(001)- 2×4 . The reason for the absence of the reflections is not due to an insufficient layer thickness, since this experimental observation is even found for films with an average thickness of $1 \mu\text{m}$. Also, the AFM images show the characteristic features of PHP films irrespective of the film thickness. As an example, we show a representative AFM image of a $1\text{-}\mu\text{m}$ -thick film in Fig. 4. The reason why we cannot observe any reflections is also not due to an amorphous film because the orientation and the well-defined island shape of PHP prove the crystalline state of the material. The absence of the reflections is, therefore, attributed to the reflection conditions of the (010)-oriented PHP layer, which should produce $0k0$ -reflections in $\theta/2\theta$ scans. However, according to this model, it is not possible to observe any reflections that are not superimposed by substrate peaks. The reflections of the PHP planes parallel to the substrate surface, which fulfil Bragg's law in $\theta/2\theta$ scans, exactly match the substrate peaks or have zero intensities. This is the case for $0k0$ -reflections, calculated from structural data for PHP given by Baker et al. [18]. The same result is deduced from our model. Reflections of the type $0k0$: $k=2n+1$ are systematically extinct due to the 2_1 axis; the intensities for the remaining reflections $0k0$: $k=2n$ have relative intensities lower than 1.5% and appear exactly at the positions of 001 peaks of the GaAs substrate. Hence, the b -axis has to be perpendicular to the GaAs(001) surface. The step height (double step) of GaAs, which corresponds to the cubic lattice parameter ($a=5.653 \text{ \AA}$), is only 1.5% larger than the double layer of PHP ($b=5.568 \text{ \AA}$). This small difference can be easily compensated by the organic material. Steps on the GaAs(001) surface, which must occur frequently because of the 2° misorientation in

$\langle 110 \rangle$, should attract and absorb PHP molecules. The coincidence of the three-dimensional growth mode and the identical height of the PHP and the GaAs steps leads to a comfortable migration of PHP across substrate and adlayer step edges.

The As-rich GaAs(001)- 2×4 surface is characterized by occurrence of additional As-dimers in the topmost layer. These dimers are oriented in a [110] direction. Therefore, one may assume a similar adsorption site for the PHP molecules. Indeed, the alignment of PHP molecules in $\langle 110 \rangle$ is clearly favored because the distance between two adjacent molecules projected in (010) is 4.0 \AA , a value that exactly corresponds to d_{110} of GaAs.

The only difference between our model and the refined crystal structure of PHP is the arrangement of the long molecule axes. In order to center the six phenyl rings on six GaAs surface units, one PHP molecule has to be shifted by about 3 \AA in axis direction $\langle 110 \rangle$ with respect to the adjacent molecule, as shown in Fig. 3a. Note, one phenyl ring fits nicely into on GaAs surface unit. With this arrangement, the formation of straight and long faces perpendicular to [100] and [010] is naturally explained. Moreover, the short faces are more random: they are located perpendicular to $\langle 710 \rangle$, forming an angle of about 8° to $\langle 100 \rangle$, and give rise to rough step edges. This behavior is observed for all islands of our AFM images.

For this model, the monoclinic PHP unit cell (space group $P2_1/c$) has different dimensions: $a=19.986 \text{ \AA}$, $b=5.653 \text{ \AA}$, $c=11.306 \text{ \AA}$ and $\beta=98.13^\circ$. The packing of the molecules is not as close as in the original cell, but the difference is less than 8%. This small difference for the whole three-dimensional unit cell is expected to be easily compensated by PHP.

Although we are aware that the proposed model is more or less speculative, it accounts for all of our experimental observations. The reliability of our model is supported by models of other groups. In particular, a growth study of PHP on to different substrates under high-vacuum conditions [19] led to the formation of a similar phase of PHP. This phase II has different a and c lattice parameters than our model and that of Baker et al. [18], and the molecules are suspected to be slightly shifted against each other. The unit cell volume is

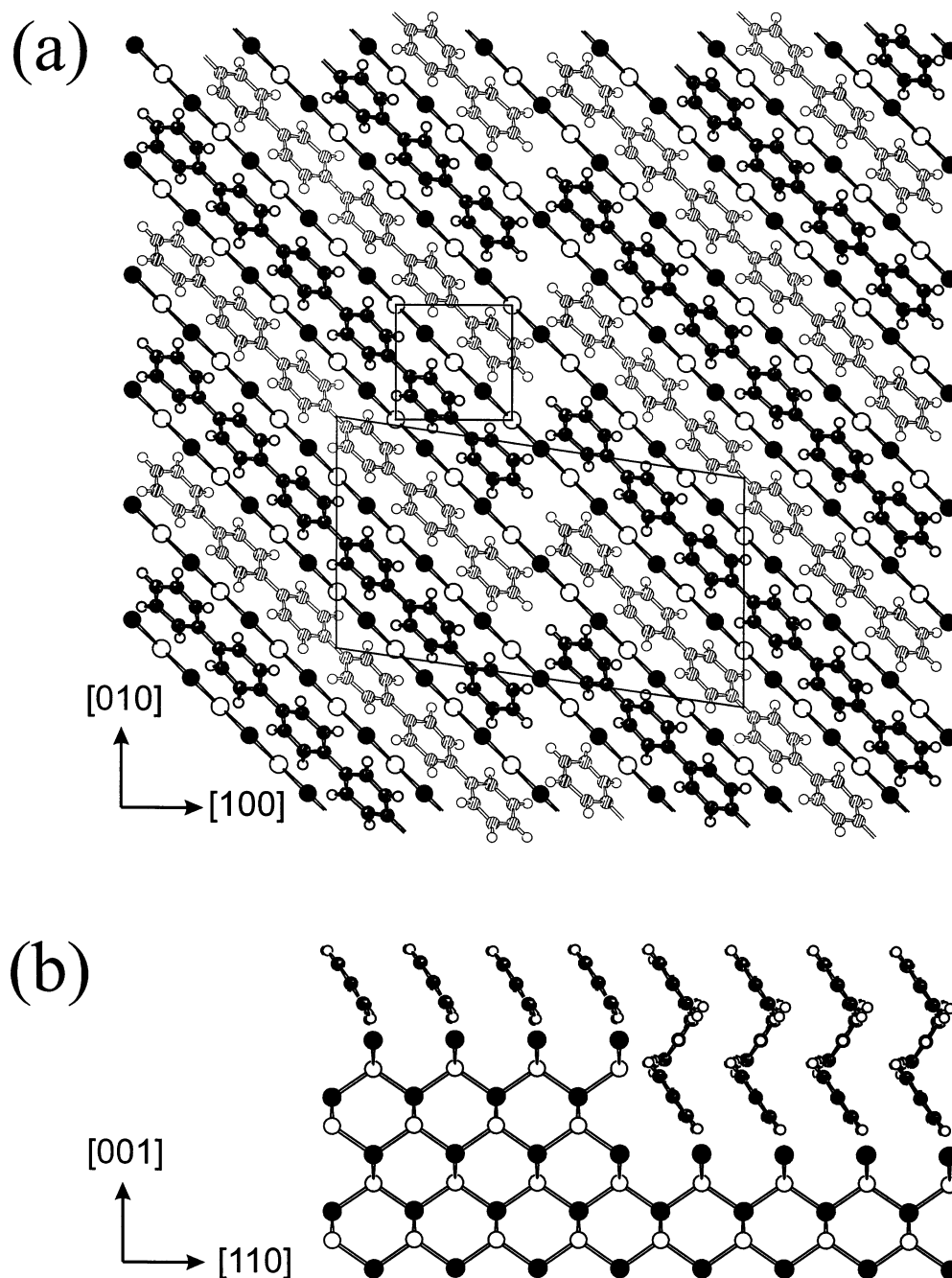


Fig. 3. Novel structural model for PHP on GaAs(001), top view (a) and side view (b). The large filled and open circles represent the gallium and arsenic atoms, respectively. It is difficult a priori to find out which kind of atoms forms the interface layer, but for this model, a determination is not necessary. The smaller filled and shaded circles represent the carbon atoms within PHP of the first and second layer. Together, they form a double layer with a height identical to the step height of a GaAs(001) double layer. The small open circles represent hydrogen. The surface unit cells of PHP and GaAs are indicated. One can clearly see the excellent lattice matching in three dimensions and the occurrence of well-defined, straight step edges along $\langle 100 \rangle$.

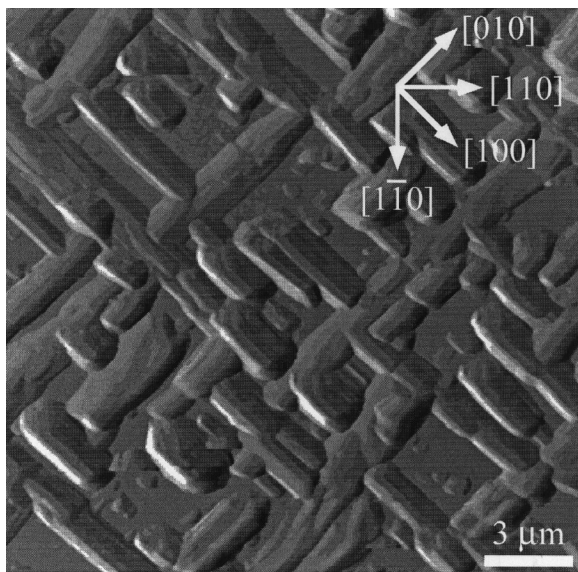


Fig. 4. AFM image of a 1- μm -thick PHP film on GaAs(001). This image was measured in differential mode, i.e. the derivative of the lines of constant force was recorded, and the islands appeared to be illuminated from the left-hand side. The sample was grown at a deposition rate of 0.7 \AA s^{-1} and a deposition time of 4 h. The substrate temperature, initially at 110°C , was increased to 150°C after 5 min.

the same as in our model within the error bars, but larger than that of Baker et al. [18].

Unfortunately, the $\theta/2\theta$ X-ray diffraction measurements cannot be used to distinguish between the original structure of Baker et al. [18], phase II proposed by Athouel et al. [19], and our model since only $0k0$ reflections are detected, and the b lattice parameter is identical for the three models. The occurrence of the phase II found by Athouel et al. [19] proves, however, that different packings with slightly shifted long axes of the PHP molecules are possible. Our model, in turn, is based on such a shift and results in the formation of straight and long $\langle 100 \rangle$ faces as observed in the AFM images.

5. Arrhenius behavior of the island density

The variation of island density with substrate temperature is demonstrated in the AFM images of Fig. 5. In this series of experiments, both depos-

ition rate (0.7 \AA s^{-1}) and deposition time (600 s) are fixed. The images show that the island density of the PHP islands varies over about two orders of magnitude when the substrate temperature is changed from 90 to 170°C . This temperature dependence of island density is quantitatively shown in Fig. 6 by an Arrhenius representation. The decrease in island density directly reflects the mobility of the PHP molecules on GaAs(001), which depends exponentially on substrate temperature. Since all data (between 90 to 170°C) are on a straight line in the Arrhenius plot, the changes in island density can be described by a single activation energy. The related fit yields an effective activation barrier of $(0.90 \pm 0.40) \text{ eV}$. In comparison with migration barriers of simple metal or semiconductor systems [22–26], this value is quite high, especially since the interactions for organic materials are believed to be small [27]. However, if we take into consideration the energy per atom, the activation barrier becomes reasonable.

The physical interpretation of this effective activation barrier is extremely complicated because of the unknown migration processes which include the crossing of step edges. In particular, one has to take into consideration the highly anisotropic shape of the PHP molecule. Nevertheless, the island density shows the well-known Arrhenius behavior, which may be used to tailor the mean island size and the island density.

6. Scaling of the island size distribution

For many inorganic homo- and heteroepitaxial systems, island size distributions have been analyzed. It has been shown that the size distributions scale with the mean island size within certain substrate temperature intervals (and fixed deposition rate). The reason for this scaling behavior is the constance of the size of the critical nucleus within such a temperature interval. The critical nucleus is closely related to the stability of the islands. This corresponds to an island that becomes stable by the incorporation of an extra atom. Stable means that the island has a higher probability of growing than dissociating during depos-

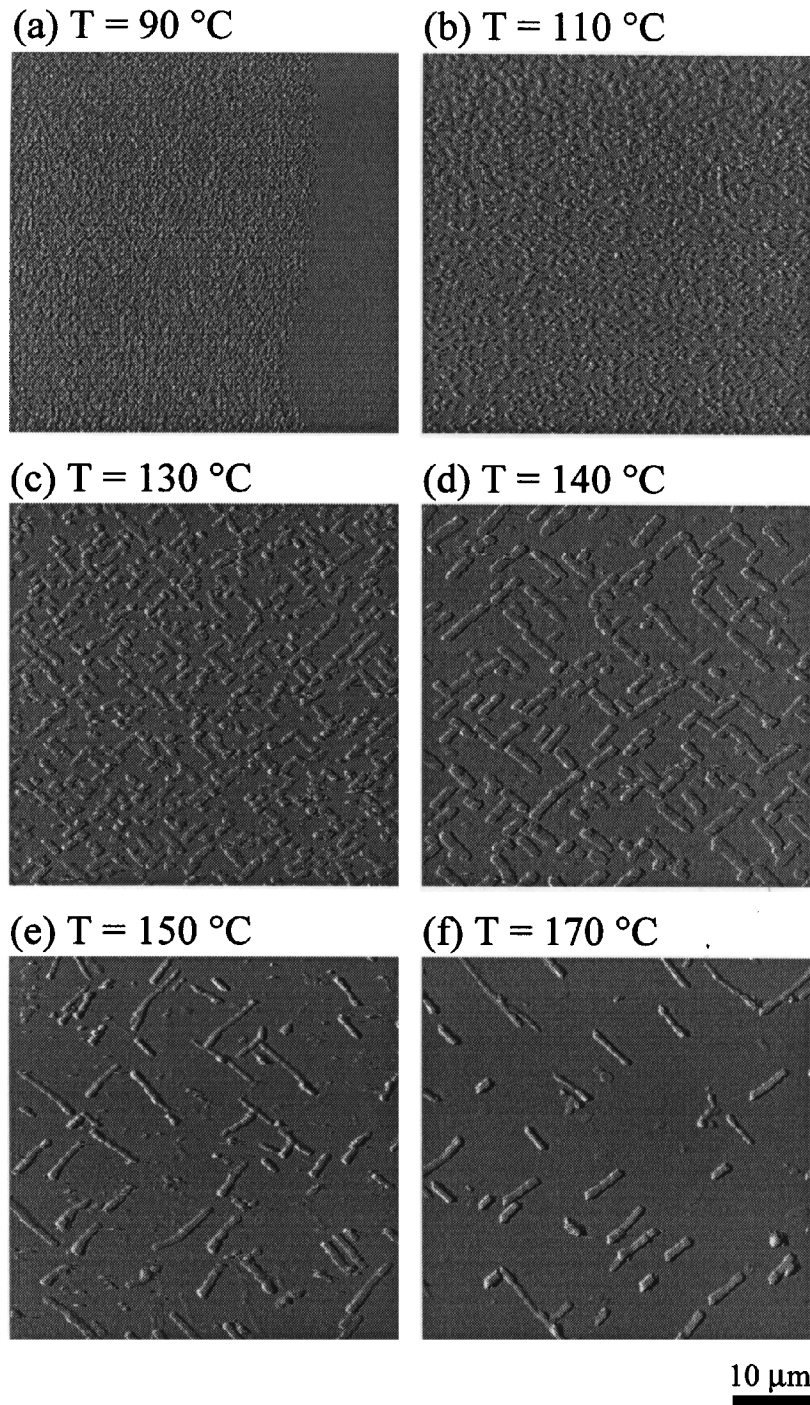


Fig. 5. AFM images characterizing the three-dimensional growth of rectangular PHP islands on GaAs(001) at different substrate temperatures. The deposition flux (0.7 \AA s^{-1}) and deposition time (600 s) were kept constant. The substrate temperatures are indicated.

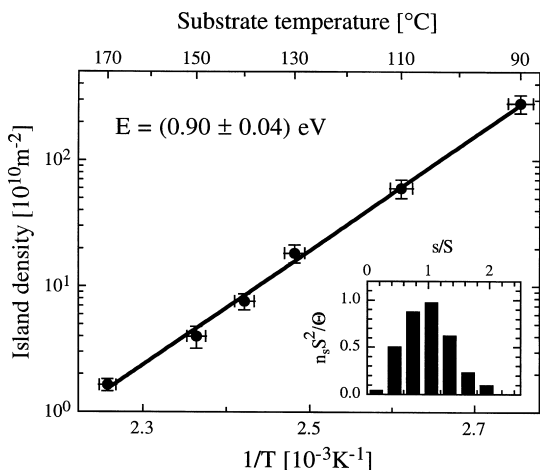


Fig. 6. Arrhenius plot of the measured island density of PHP/GaAs(001). Inset: Scaled island size distribution deduced from AFM images at different substrate temperatures (110, 130, 140, 150, and 170°C). The island size distribution, n_s , corresponds to the density per site of islands containing s molecules at coverage θ , and S is the average island size at fixed coverage. s/S is the scaled island size, i.e. the island size relative to the average island size, so that the size distributions collapse into one curve (for growth conditions, see Fig. 5).

ition. Both theoretical studies and experiments show that the scaled island size distributions are characteristic for the size of the critical nucleus. Therefore, it is possible to determine the size of the critical nucleus just by a comparison of the experimental data with simulations based on scaling theory.

To our knowledge, there are no studies of the scaling behavior for organic islands on inorganic semiconductor surfaces. This may arise from the question of whether the concept of the critical nucleus is applicable for such large molecules. Cluster deposition experiments, however, have convinced us to assume the validity of the concept [28]. More important was the question of whether the scaling behavior can be found in the investigated substrate temperature range. That would support the assumption of a single activation barrier for the Arrhenius plot in Fig. 6. Indeed, we have found that the scaled island size distributions are identical (within the error bars given by the statistics: $\Delta(n_s S^2 / \theta) = 0.04$ for the substrate temperatures of 110, 130, 140, 150, and 170°C where an analysis was convenient. The average data are

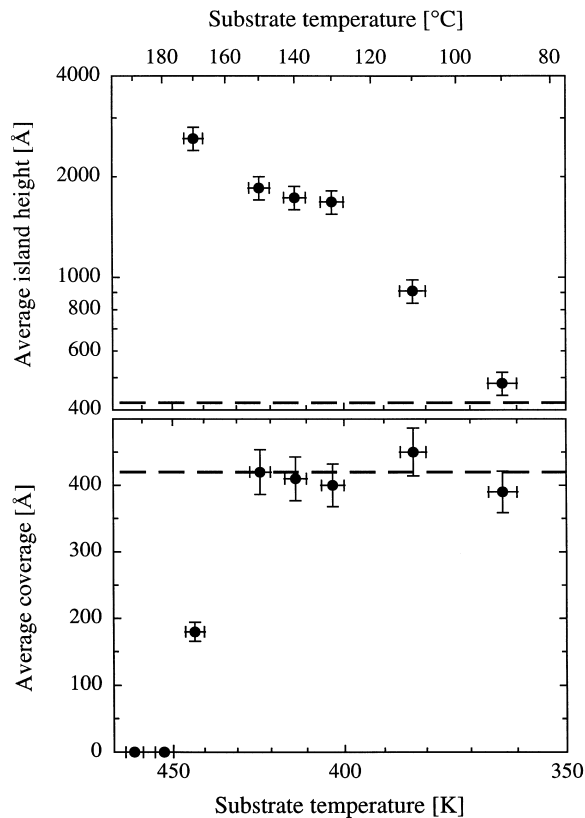


Fig. 7. Quantitative analysis of three-dimensional PHP islands on GaAs(001). Plotted are the average island height (logarithmic scale) and average film thickness (linear scale) of PHP versus substrate temperature. The dashed line corresponds to the average coverage without desorption.

presented as an inset in Fig. 6. For our system, it is irrelevant whether the size of the three-dimensional island or just the two-dimensional area of the islands is considered. Both exhibit the same scaling behavior. This conclusion becomes evident comparing the data of Figs. 6 and 7 (upper part). Within the temperature range of 90 to 170°C, the average island height is increased by a factor of 6. If the size of the two-dimensional island grows with the same ratio, i.e. by a factor of 36, the mean island size should increase by a factor of 210, which would correspond to a reduction in island density by a factor of 210, as shown in Fig. 6.

A comparison with theoretical data based on scaling theory [29,30] should yield the size of the

critical nucleus. The scaled island size distributions for PHP/GaAs(001) have a maximum of less than one at the mean island size and a tail exceeding the double value of the scaled island size s/S . Such a broad distribution is characteristic of small critical nuclei. It corresponds rather to a critical nucleus $i^* = 1$ than to $i^* = 2$, indicating that individual PHP molecules can migrate, whereby a dimer forms a stable island. Note, the size of the critical nucleus can be quite small whereby the islands may contain, for example, 10^6 molecules.

The island size distributions may be influenced by desorption effects. At elevated substrate temperatures, the sticking coefficient becomes low, and the molecules can desorb from the surface, resulting in a reduced film thickness. Due to the high density of single molecules on the surface during the deposition experiment, desorption will start at much lower substrate temperatures than sublimation. [Note the difference between adatom (single molecule) desorption and sublimation at equilibrium: the latter requires an atom or molecule to be extracted from a kink site on a step edge, e.g. for a (001) face of a cubic lattice, three bonds have to be broken. Desorption of an adatom, however, just costs the energy of one broken bond. Hence, desorption of single molecules results in a much higher rate at a given substrate temperature.] Using the AFM images, we have measured the average coverage of PHP as a function of substrate temperature. As shown in the lower part of Fig. 7, we find a constant average value for the film thickness up to 150°C , a significantly reduced value at 170°C , and the bare substrate at 180°C and 190°C . This means that desorption of PHP molecules from GaAs(001) does not play an important role for scaling of the island size distribution.

7. Interpretation of the island shape

The AFM images in Figs. 1 and 5 show a constant width of the rectangular-shaped islands. This constant island width is a special feature of coherently strained epitaxial islands in heteroepitaxial growth. Tersoff and Tromp [31] have theoretically predicted a strain-induced spontaneous shape transition from two-dimensional to one-

dimensional growth of flat islands with a rectangular basis. This means that three-dimensional islands with a height much smaller than their width and length grow to a critical size in both [100] and [010]. Above the critical size, the islands grow in length but not in width. The width even shrinks by a factor of $e \approx 2.7$ and reaches an asymptotic value. We have observed this asymptotic island width within each individual AFM image where the islands are large enough (e.g. cp. Fig. 5e). Smaller islands are slightly wider, as can be seen in Fig. 5d. This ratio is smaller than a factor of e , but the experimental data show the right tendency. The islands grow not only in length but also in height, an experimental detail that is not considered in this simple theory. The upper part in Fig. 7 demonstrates the exponential increase in height with substrate temperature. Although the width of the islands slightly differs from image to image due to tip changes, one can definitely conclude that PHP/GaAs(001) is a prominent example, which gives evidence for the theory of Tersoff and Tromp.

8. Conclusion

In conclusion, we have demonstrated that PHP grown on GaAs(001)- 2×4 forms well-defined epitaxial coherently strained islands. Although the island height increases with substrate temperature, we have found another example for the Tersoff–Tromp theory of island shape transition in coherently strained island growth. The island density, which shows the well-known Arrhenius behavior, and the scaled island size distribution are identical to simple atomic systems. This means that the concept of crystal growth, i.e. nucleation and scaling theory, should be quite general. Nevertheless, the nature of the deduced quantities, such as the activation barrier of 0.9 eV, are not clear, and further studies are necessary to determine the fundamental migration and nucleation processes. The growth of PHP/GaAs(001) is part of the first quantitative studies of organic molecules on well-prepared inorganic semiconductor surfaces, and constitutes a starting point for further experiments. We are convinced that PHP/GaAs

(001) is not the exception. A similar type of island growth in two perpendicular directions was reported, for example, for *n*-tritracontane on KCl substrates [32].

References

- [1] S. Tasch, C. Brandstätter, F. Meghdadi, G. Leising, G. Froyer, L. Athouel, *Adv. Mater.* 9 (1997) 33.
- [2] H. Yanagi, S. Okamoto, *Appl. Phys. Lett.* 71 (1997) 2563.
- [3] B. Müller, Research Report, AG Quantenmikrostrukturen, TU Dresden, 1988.
- [4] L. Däweritz, R. Hey, *Surf. Sci.* 236 (1990) 15.
- [5] W. Mönch, *Semiconductor Surfaces and Interfaces*, 2nd ed., Springer, Berlin, 1995.
- [6] J. Behrend, PhD thesis, Humboldt-University, Berlin, 1996.
- [7] A.R. Avery, H.T. Dobbs, D.M. Holmes, B.A. Joyce, D.D. Vvedensky, *Phys. Rev. Lett.* 79 (1997) 3938.
- [8] C. Chevrot, M.T. Riou, F. Froyer, *Synth. Met.* 55–57 (1993) 4783.
- [9] I.C. Lewis, J.B. Barr, *Mol. Cryst. Liq. Cryst.* 72 (1981) 65.
- [10] P.A. Irvine, D.C. Wu, P.J. Flory, *J. Chem. Soc., Faraday Trans.* 80 (1984) 1795.
- [11] R. Resel, N. Koch, F. Meghdadi, G. Leising, W. Unzog, K. Reichmann, *Thin Solid Films* 305 (1997) 232.
- [12] J.A. Venables, G.D.T. Spiller, M. Hanbücken, *Rep. Prog. Phys.* 47 (1984) 399.
- [13] A. Gustafsson, D. Hessman, L. Samuelson, J.F. Carlin, R. Houdre, A. Rudra, *J. Cryst. Growth* 147 (1995) 27.
- [14] R.R. Chance, A. Prock, R. Silbey, *Adv. Chem. Phys.* 37 (1978) 1.
- [15] M. Klemenc, F. Meghdadi, S. Voss, G. Leising, *Synth. Met.* 85 (1997) 1243.
- [16] M. Klemenc, Diploma thesis, Graz University of Technology, Austria, 1997.
- [17] E. Zojer, M. Knupfer, R. Resel, F. Meghdadi, G. Leising, J. Fink, *Phys. Rev. B* 56 (1997) 10138.
- [18] K.N. Baker, A.V. Fratini, T. Resch, H.C. Knachel, W.W. Adams, E.P. Socci, B.L. Farmer, *Polymer* 34 (1993) 1571.
- [19] L. Athouel, G. Froyer, M.T. Riou, M. Schott, *Thin Solid Films* 274 (1996) 35.
- [20] J.A. Stroschio, D.T. Pierce, *Phys. Rev. B* 49 (1994) 8522.
- [21] B. Müller, B. Fischer, L. Nedelmann, H. Brune, K. Kern, *Phys. Rev. B* 54 (1996) 17858.
- [22] Y.W. Mo, J. Kleiner, M.B. Webb, M.G. Lagally, *Phys. Rev. Lett.* 66 (1991) 1998.
- [23] B. Voigtländer, A. Zinner, *Surf. Sci.* 292 (1993) L775.
- [24] M. Horn-von Hoegen, H. Pietsch, *Surf. Sci.* 321 (1994) L129.
- [25] B. Voigtländer, A. Zinner, T. Weber, H.P. Bonzel, *Phys. Rev. B* 51 (1995) 7583.
- [26] B. Müller, M. Henzler, *Surf. Sci.* 389 (1997) 338.
- [27] S.R. Forrest, *Chem. Rev.* 97 (1997) 1793.
- [28] L. Bardotti, P. Jensen, A. Hoareau, M. Treilleux, B. Cabaud, A. Perez, F. Cadete Santos Aires, *Surf. Sci.* 367 (1996) 276.
- [29] M.C. Bartelt, J.W. Evans, *Phys. Rev. B* 46 (1992) 12675.
- [30] G. Amar, F. Family, *Phys. Rev. Lett.* 74 (1994) 2066.
- [31] J. Tersoff, R.M. Tromp, *Phys. Rev. Lett.* 70 (1993) 2782.
- [32] K. Matsushige, T. Hamano, T. Horiuchi, *J. Cryst. Growth* 146 (1995) 641.